JCB Article

Targeted ablation of *NrCAM* or *ankyrin-B* results in disorganized lens fibers leading to cataract formation

Margret I. Moré, Frank-P. Kirsch, and Fritz G. Rathjen

Max-Delbrück Center for Molecular Medicine, D-13092 Berlin, Germany

The NgCAM-related cell adhesion molecule (NrCAM) is an immunoglobulin superfamily member of the L1 subgroup that interacts intracellularly with ankyrins. We reveal that the absence of NrCAM causes the formation of mature cataracts in the mouse, whereas significant pathfinding errors of commissural axons at the midline of the spinal cord or of proprioceptive axon collaterals are not detected. Cataracts, the most common cause of visual impairment, are generated in NrCAM-deficient mice by a disorganization of lens fibers, followed by cellular disintegration and accumulation of cellular debris. The disorganization of fiber cells becomes histologically distinct during late embryonic development and includes abnormalities of the cytoskeleton and of connexin50-containing gap junctions. Furthermore, analysis of lenses of ankyrin-B mutant mice also reveals a disorganization of lens fibers at postnatal day 1, indistinguishable from that generated by the absence of NrCAM, indicating that NrCAM and ankyrin-B are required to maintain contact between lens fiber cells. Also, these studies provide genetic evidence of an interaction between NrCAM and ankyrin-B.

Introduction

The transmembrane glycoprotein NgCAM-related cell adhesion molecule (NrCAM)* is a member of the L1 subgroup of immunoglobulin (Ig)-like cell adhesion proteins. This subgroup is composed of NrCAM, neurofascin, close homologue of L1 (CHL1), and L1 itself in vertebrates, and neuroglian and tractin in invertebrates (Brümmendorf et al., 1998; Hortsch, 2000). Like L1, NrCAM contains six Ig-like domains and five fibronectin type III (FNIII)-like repeats, a hydrophobic stretch, and a highly conserved cytoplasmic segment (Grumet et al., 1991; Kayyem et al., 1992). A crucial role of the L1 subgroup of proteins in neural development is exemplified by a broad spectrum of neuroanatomical and neurological disorders caused by the knock out of the murine L1 gene (Dahme et al., 1997; Cohen et al., 1998; Demyanenko et al., 1999) and by mutations in the human L1 gene that affect the binding activity and trafficking of L1 (De Angelis et al., 1999; Moulding et al., 2000). As also shown for other L1 subgroup members, NrCAM reveals a complex homo- and heterophilic binding pattern and is implicated in cell–cell contact processes (Mauro et al., 1992). In in vitro bioassays it can promote axonal growth by binding to neurofascin, F11, or receptor protein tyrosine phosphatase (RPTP)β/ζ (Morales et al., 1993; Volkmer et al., 1996; Sakurai et al., 1997) and can mediate interactions between neurons and glial cells via axonin-1 (Suter et al., 1995). In ovo antibody perturbation experiments indicate that NrCAM is important for commissural axons of the chicken spinal cord to grow across the midline through the floor plate and for proprioceptive axon collaterals to extend ventrally within the spinal cord (Stoeckli and Landmesser, 1995; Fitzli et al., 2000; Perrin et al., 2001). NrCAM has also been found to be expressed specifically at the node of Ranvier in rat where it interacts with the cytoskeletal adaptor protein ankyrin-G (Lambert et al., 1997). Binding to ankyrin appears to be a common feature of L1 subfamily members and requires a highly conserved sequence within their cytoplasmic tails (Davis and Bennett, 1994). This interaction appears to be inhibited by tyrosine phosphorylation as demonstrated for neurofascin (Tuvia et al., 1997), whereas clustering of the L1 subfamily member neuroglian at adhesion sites activates ankyrin binding followed by a redistribution of spectrin (Jefford and Dubreuil, 2000).

In this paper, we describe the generation of *NrCAM* knock-out mice by gene targeting. The mice are viable and fertile, but smaller than heterozygous or wild-type littermates, and they show a slight motor defect. Although

Address correspondence to Fritz G. Rathjen, Max-Delbrück-Center für Molekulare Medizin, Robert-Rössle-Strasse 10, D-13092 Berlin, Germany. Tel.: 49-30-9406-3709. Fax: 49-30-9406-3730. E-mail: rathjen@mdc-berlin.de

*Abbreviations used in this paper: CHL1, close homologue of L1; ES, embryonic stem; FNIII, fibronectin type III; HE, hematoxylin/eosin; Ig, immunoglobulin; NrCAM, NgCAM-related cell adhesion molecule; PFA, paraformaldehyde; RT, room temperature; RPTP, receptor protein tyrosine phosphatase; TB, toluidine blue.

Key words: cell adhesion; Ig superfamily; L1 subgroup; cataract; axon outgrowth

The Journal of Cell Biology, Volume 154, Number 1, July 9, 2001 187–196
http://www.jcb.org/cgi/doi/10.1083/jcb.200104038

$NrCAM^{-/-}$ neurons, unlike wild-type, are unable to grow on neurofascin and F11 in cell culture, $NrCAM^{-/-}$ mice have no significant abnormalities on a histological level in any of their neural tissues. Also, unexpectedly, their commissural axons cross the spinal cord midline normally. Interestingly, we observed cataract formation due to a loss of intercellular communication between lens fiber cells followed by disintegration of cells. A similar disorganization of lens fiber cells was also observed in ankyrin-B–deficient mice. These observations suggest that NrCAM and ankyrin-B–deficient mice might provide further insights into cataractogenesis, one of the most common causes of visual impairment (Francis et al., 1999, 2000; Graw, 1999).

Results

The NrCAM locus and derivation of mutant mice

To study the function of NrCAM in an in vivo situation, we generated a mouse strain deficient for this gene. To do this, we first characterized the *NrCAM* locus surrounding the ATG using a mouse embryonic stem (ES) cell BAC clone. A long and a short arm was subcloned from the BAC clone to construct the targeting vector to destroy the start codon within exon 4 (Fig. 1 a). Electroporated ES cells were screened for homologous recombination and used to create chimeric mice via blastocyst injection. The correct integration of the targeting vector and a deletion of the ATG-containing exon was confirmed by Southern hybridization as shown in Fig. 1 b and using the PauI-NheI fragment (region deleted in the mutant) as probe (not shown). Alternatively, the replacement of the ATG-containing exon by the neo cassette in the mutant mice was shown by PCR (Fig. 1 c). To detect NrCAM at the protein level, we generated polyclonal antibodies against a glutathione *S*-transferase fusion protein of the FNIII domains 1–4 of NrCAM. Immunohistochemical studies and an immunoblot from brains of both wild-type and NrCAM-deficient mice (Fig. 1 d; not shown) show the absence of NrCAM in the mutants.

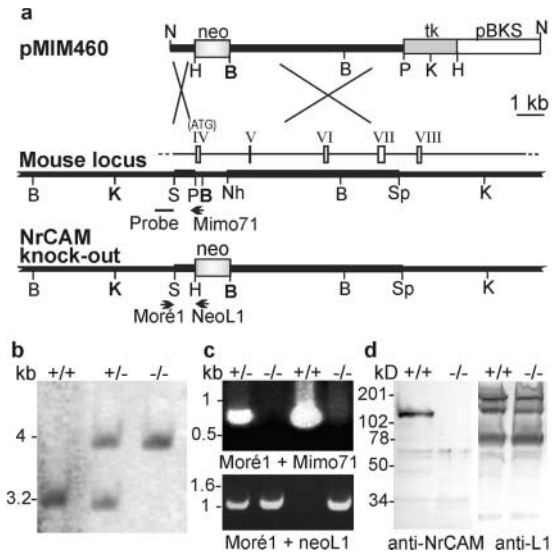

Figure 1. **NrCAM gene disruption.** (a) Map of the targeting vector, and of part of the genomic locus before and after homologous recombination with the targeting vector. The position of exons 5, 6, and 8 as well as the exon numbering was adopted from the human NrCAM locus (Dry et al., 2001). neo, PGKneopA cassette; tk, MC1TKpA cassette; H, HindIII; K, KpnI; S, SacI; P, PauI; B, BamHI; N, NheI; Sp, SpeI. Only relevant restriction sites are shown. The positions of the external Southern blot probe, as well as the PCR primers, are indicated. (b) Southern blot of DNA from tail biopsies of wild-type, heterozygous, and homozygous mice, using the restriction enzymes BamHI and KpnI. (c) PCR of genomic DNA using the primers Mimo71 and Moré1 (c), and the primers neoL1 and Moré1. (d) Immunoblot blot analysis using whole brain from adult wild-type and $NrCAM^{-/-}$ mice using polyclonal antibody 463 against NrCAM. The NrCAM band is completely absent in the mutants. Additional bands are due to nonspecific binding activity of the antibody. To demonstrate equal loading, a parallel blot was analyzed with polyclonal antibodies to L1. Molecular weight markers are indicated on the left. Immunohistological studies using neural tissue as well as immunoblots of brain and lens tissue using a polyclonal antibody provided by M. Grumet also reveal that NrCAM is absent (not shown).

NrCAM-deficient mice develop a mature cataract

NrCAM-deficient mice are viable and fertile. Although the gross anatomy of the nervous system appears normal, mutant mice develop a mature cataract in their lenses that becomes visible from the outside of the eye after 4 mo of age (Fig. 2 c). This cataract development was found to be progressive: 1-mo-old mice had lenses that were slightly less translucent in the nuclear region than wild-type lenses, and 4-mo-old mice already had a white opaque lens center. 9-mo-old mice had completely opaque lenses (Fig. 2 a). However, we could observe some variance in the degree of opacity and size as demonstrated by the comparison of lenses of several 11-mo-old $NrCAM^{-/-}$ siblings (Fig. 2 b; compare also 4-mo-old lenses in Fig 2 a). Upon piercing mutant cataract lenses with forceps, material was extruded, indicating liquefication of secondary lens fibers. After removal of the lens capsule and its adhering tissue, only the hardened interior of primary lens fibers remained, looking not transparent like in wild-type but whitish, with an irregular surface. All adult NrCAM-deficient mice examined to date had a cataract indicating a penetrance of 100%.

In addition to cataract formation, NrCAM deleted mice are slightly smaller and show a slight impairment of their motor abilities. To analyze the occurrence of the growth deficit, we followed the weights of 12 littermates during postnatal development (Fig. 2 d). At birth, most $NrCAM^{-/-}$ mice were already relatively lighter than their heterozygous littermates and, at postnatal day (P)9.5, all NrCAM-deficient mice were lighter than their same-sexed heterozygous control siblings. At P15 to P35, the weight differences were most apparent; however, mutant animals stayed at ~80% of the weight of their control siblings for their entire lifetime (not shown). To analyze whether the absence of NrCAM had an effect on the motor ability, we tested female NrCAM-deficient mice and wild-type control mice of similar weight for their ability to stay on a motionless or rotating rotarod. Generally, mutant mice fell from the rod at a higher frequency, especially when the rod was moving (Fig. 2 e).

Localization of NrCAM in the lens

NrCAM has been studied so far primarily in the developing nervous system. To investigate its function in the formation

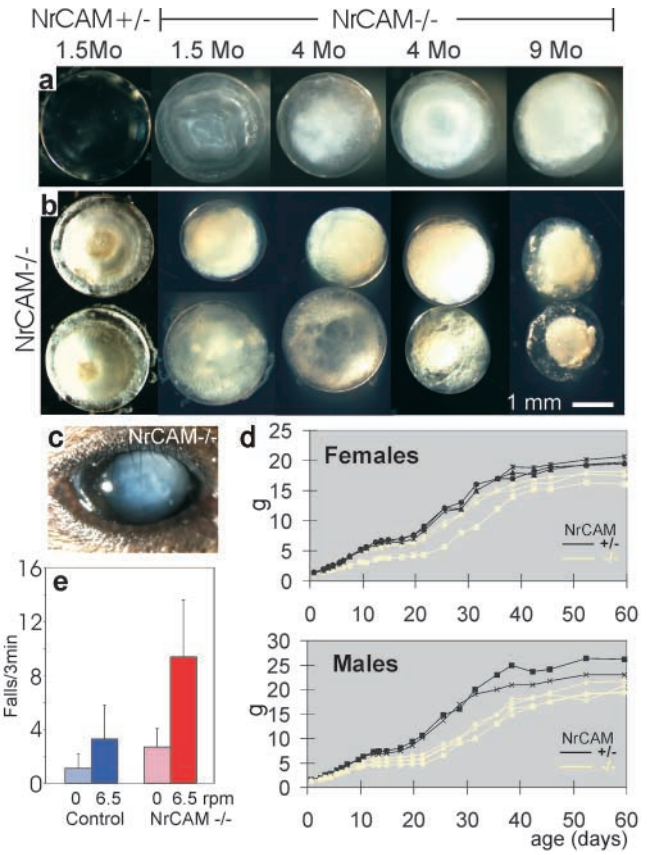

Figure 2. **NrCAM-deficient mice develop cataracts and reveal reduced body weight and motor disabilities.** (a) Stages of cataract development. From left to right: 1.5-mo-old NrCAM$^{+/-}$ lens; NrCAM$^{-/-}$ littermate; both lenses from 4-mo-old NrCAM$^{-/-}$ mouse; 9-mo-old NrCAM$^{-/-}$ lens; same magnification as in b. (b) Lens pairs from 11-mo-old NrCAM$^{-/-}$ siblings. (c) Eye of a freshly killed 4-mo-old NrCAM mouse. (d) Weights of NrCAM$^{+/-}$ and NrCAM$^{-/-}$ littermates during postnatal development. Black line and symbols, NrCAM$^{+/-}$ animals; light line and symbols, NrCAM$^{-/-}$ animals. (e) Rotarod test. The number of times the animals fell from the rod in 3 min is indicated for a nonmoving rod and the rod rotating with 6.5 rpm. Each animal was confronted without prior rod experience, first with the nonmoving rod, and after a recovery time, with the rotating rod.

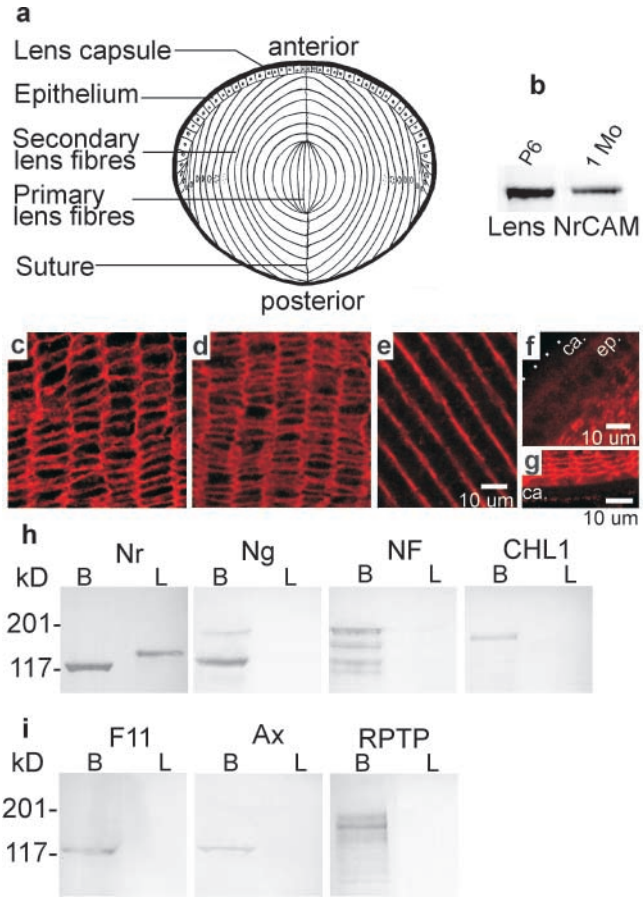

Figure 3. **Expression of NrCAM in lens.** (a) Schematic overview of an adult mouse lens as central longitudinal section. The lens has a spheric shape with a symmetry around its rotational axis. It contains primary lens fibers that are formed during early embryonic development and secondary lens fibers that are formed during later embryonic development and throughout life. The anterior end (pointing upwards) has a monolayer of epithelial cells that can divide and migrate towards the sides of the lens, followed by an elongation and maturation process, in which the nucleus and other organelles are lost and characteristics of secondary fiber cells are adopted. For clarity, the capsule, epithelial cells, and lens fibers are not drawn to scale (adapted from Bassnett et al., 1999). (b) Immunoblot of mouse lens proteins using 463 polyclonal antibody against NrCAM. Proteins of lenses from animals aged as indicated are loaded. (c–e) Same magnification. (c) Noncentral longitudinal section through 9-mo-old wild-type mouse secondary lens fibers stained with polyclonal antibodies against NrCAM. (d) E14 chick noncentral longitudinal lens section stained with monoclonal antibody number 3 against chick NrCAM. (e) E14 chick lens longitudinal section stained with polyclonal antibodies against NrCAM. (f and g) Mouse P12 noncentral longitudinal lens sections stained with polyclonal antibodies against NrCAM. ca., capsule; ep., epithelium. (f) side-front region with epithel. The outer edge of the capsule is marked. (g) Posterior edge of the lens. (h and i) Immunoblots of E14 brain (B) and lens (L) lysates reveal that only NrCAM, but no other family members or extracellular NrCAM interaction partner is present in the lens. Since antibodies to anti-CHL1 or anti-RPTPβ/ζ are available only for mouse proteins, these were not tested in chick. For the other proteins, the chick immunoblot is shown for reasons of availability or quality of the antibodies. Molecular weight markers are indicated on the left. (h) Expression of NrCAM, NrCAM homologues NgCAM (species homologue of mouse L1), neurofascin, and CHL1. Note that neurofascin is expressed in several molecular weight forms. (i) Expression of extracellular NrCAM interaction partners F11, axonin-1, and RPTPβ/ζ.

of cataracts, we first analyzed the distribution of NrCAM and its extracellular ligands in chick as well as in mouse lenses at various developmental stages by histological methods and Western blotting. Fig. 3 a gives an overview of the lens architecture. Antibodies against NrCAM stain the cell surface of secondary fiber cells in mouse (Fig 3 c) as well as in chick sections (Fig. 3, d and e), showing regular staining patterns depending on the direction and position of the section. The fiber cells are flattened hexagons in cross-section (Fig. 3, c and d), and the radial cell surfaces are highlighted more than the tangential cell surfaces. A longitudinal section of the mouse or chick lens results in a pattern of parallel lines, each line representing the neighboring cell surfaces of two lens fiber cells (Fig. 3 e). The expression of NrCAM in the primary lens fibers was still visible in P12 mouse lenses, but very low in adult mouse lenses (not shown). Interestingly, no NrCAM expression was observed in the lens epithelium or the lens capsule (Fig. 3 f), or the cell surface of fiber cells bordering the capsule (Fig. 3 g), indicating that the

contact formation between lens epithelial cells and between lens fiber cells and capsule is not mediated by NrCAM.

Analysis of immunoblots of lens homogenates of mice or chick reveals that NrCAM is prominently expressed in the lens during postnatal development and that the expression is reduced during adulthood (Fig. 3 b). No other L1 subfamily proteins, including the NrCAM ligand neurofascin, are expressed in the lens at any stage (Fig. 3 h). Also, other heterophilic extracellular ligands of NrCAM such as the F11 protein, axonin-1 or RPTPβ/ζ, are absent from the lens (Fig. 3 i). Interestingly, chick lens NrCAM is consistently slightly larger than chick brain NrCAM (Fig. 3 h), whereas mouse lens NrCAM has approximately the same size as the smaller of two almost comigrating bands of brain NrCAM (not shown). These size differences might be due to posttranslational modifications such as glycosylation or to alternative splicing of its pre-mRNA. In summary, the absence of the currently known NrCAM ligands suggests a homophilic binding mode of NrCAM between opposing lens fiber membranes. However, heterophilic binding of NrCAM to a so far uncharacterized membrane protein expressed on lens fibers cannot be excluded.

Histological analysis of cataract development in NrCAM-deficient mice

To begin to understand the importance of NrCAM for the development and maintenance of a functional translucent lens, we investigated lenses of NrCAM$^{-/-}$ mice of different stages by standard histological methods. In mouse lenses of E14.5 embryos that consist predominantly of primary lens fibers, no significant morphological changes were observed in the NrCAM mutant (Fig. 4 a). At E18, secondary lens fibers have developed. Even though there are roundish large-appearing cells especially at the anterior pole close to the suture in the mutant, most of the fiber cells remain ordered in the transition zone as in wild type (Fig. 4, b and c). Also, at P12 there are many fiber cells remaining in a somewhat ordered context, in particular in the periphery, but the number of rounded disoriented cells among the secondary lens fibers increases towards the nucleus of the lens (Fig. 4 d). By 2 mo, the regular wild-type pattern (Fig. 4 e) of cross-sectioned secondary lens fibers is severely disturbed in the NrCAM$^{-/-}$ lens (Fig. 4 f), as shown here for the region around the posterior pole. The cell shape and arrangement is still most ordered for the cells that have migrated inwards from the epithelium more recently (Fig. 4 g, upper right). But even among these cells, there are some cells that start to round up, becoming shorter and thicker (arrow). Other cells have lost their integrity completely, creating distinct zones of cellular debris (Fig. 4 g, *). Persisting cells are intensely stained, rounded, and have lost their orientation (Fig. 4 g, arrowhead). At regions half-way to the center of the lens, especially at the posterior region, we observe deformed cells that have lost contact to each other completely (Fig. 4 h).

At the age of 8 mo, the cataract has progressed even further. The only intact region remains the zone of inward migrating cells at the lens equator, but even these cells start to round up soon (Fig. 4 i, arrow). In Fig. 4 j, even the cells directly below the epithelium appear swollen and are in the process of losing touch with neighboring cells (compare with Fig. 4 g).

The lens now contains a large amount of liquefied cellular debris that may develop due to metabolic imbalances (Fig. 4 j). The cells towards the posterior pole (Fig. 4 k) also exhibit less integrity than in the 2-mo-old lens (compare with Fig. 4 f).

The primary lens fibers of NrCAM$^{-/-}$ mice show no abnormalities at E14 (Fig. 4 a), and only slight irregularities can be observed at P12 (not shown). In the adult, they become less ordered and less elongated than in wild type, but due to their rigidity, a solid lens nucleus is preserved (not shown).

At all stages, the lens epithelium of NrCAM$^{-/-}$ lenses appears to be normal; however, the posterior lens capsule was observed to be thinner (Fig. 4 f) than in heterozygous or wild-type controls in some cases. In contrast to cataracts caused by some other mutations, there is no vacuole formation at any stage in NrCAM$^{-/-}$ lenses. The cornea, iris, ciliary body, and retina do not show any abnormalities on a histological level (not shown).

Disorganization of lens fibers in the absence of ankyrin-B

NrCAM, as well as other L1 subfamily members, have been shown to interact with the cytoskeletal linker proteins of the ankyrin family that associate via spectrin with F-actin (Davis and Bennett, 1994; Tuvia et al., 1997; Jefford and Dubreuil, 2000). To study whether the interaction between NrCAM and ankyrin is important for the development of lens structure, we first analyzed the expression of ankyrins in lens. To date, there are three different ankyrin genes known. Western blot analysis using a polyclonal antibody against ankyrins previously revealed that lens ankyrin did not comigrate with erythrocyte ankyrin, but instead had the molecular weight as would be expected of ankyrin-B (Dola et al., 1990). Consistently, specific monoclonal antibodies confirm the presence of ankyrin-B, but not ankyrin-G, in the lens (Fig. 5 a). Examination of the staining pattern of ankyrin-B in the secondary lens fibers by immunohistological methods (Fig. 5 b) shows that the pattern of localization matches that of NrCAM (Fig. 3 c). Like NrCAM, ankyrin-B is also not expressed at the cell membranes of fiber cells contacting the capsule, nor in the capsule itself (Fig. 5 d); however, ankyrin-B is expressed in the epithelial cells (Fig. 5 c). This localization of ankyrin-B makes an interaction between these two proteins in lens fiber cells likely.

For this reason, we reanalyzed whether ankyrin-B$^{-/-}$ mice previously generated (Scotland et al., 1998) also develop a disorganized lens. Since most ankyrin-B$^{-/-}$ mice do not survive beyond P1, we had to analyze the lenses of ankyrin-B$^{-/-}$ mice at this stage. Interestingly, the organization of secondary lens fibers at the anterior pole was severely disturbed in the ankyrin-B$^{-/-}$ lenses (Fig. 6, a and b), closely resembling the lenses of NrCAM$^{-/-}$ mice at a similar stage (Fig. 4, b and c). In contrast, the lenses of control siblings revealed an ordered arrangement of lens fibers (Fig. 6, c and d). Even though the lens epithelium strongly expresses ankyrin-B, its absence had no significant effect on the organization of epithelial cells. The observation that the absence of the cytoskeletal linker protein ankyrin-B results in a disorganization of lens fiber cells similar to that observed in the absence of NrCAM suggests that NrCAM mediated cell–cell contact between lens fibers requires a direct link to the actin cytoskeleton.

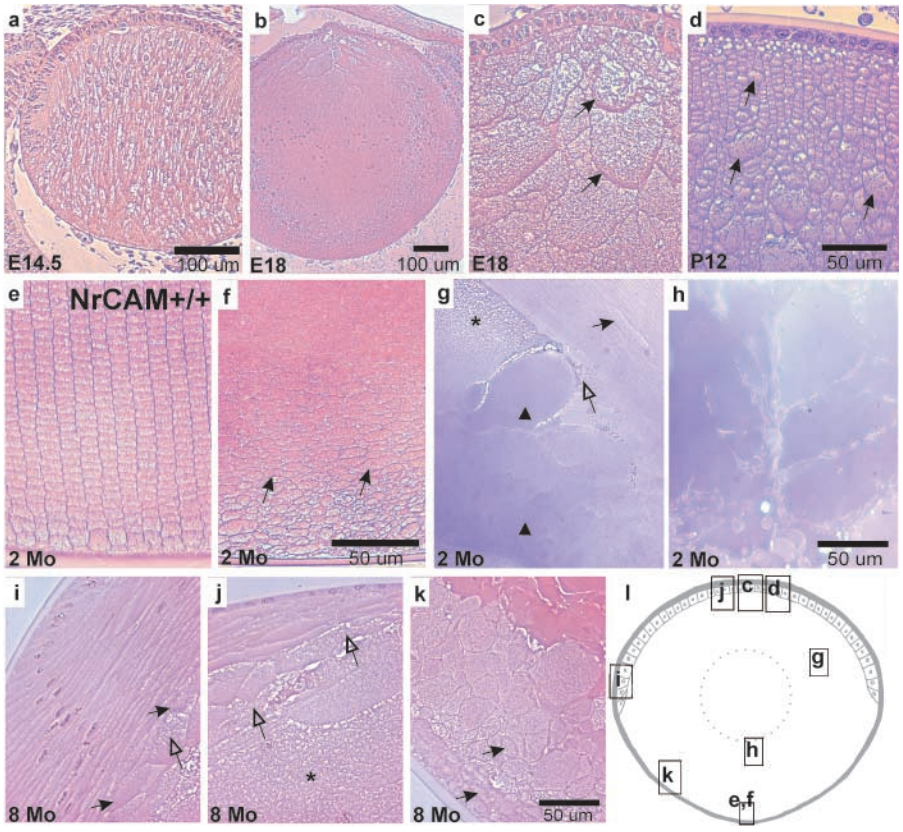

Figure 4. **Cataract histology of NrCAM-deficient mice.** From the emergence of secondary lens fibers onwards, NrCAM-deficient lens fibers develop a rounded instead of elongated shape, indicating loss of cell–cell contact. The phenotype is progressive and leads to a disintegration of lens fibers and accumulation of cellular debris. (a) NrCAM$^{-/-}$ E14.5 longitudinal section, HE stained. (b and c) NrCAM$^{-/-}$ E18 longitudinal sections, HE stained. (d) NrCAM$^{-/-}$ P12 noncentral longitudinal section, anterior region, TB stained. (c–k) Positions of sections in the lens are indicated in l. (e) 2-mo-old wild-type posterior region in noncentral longitudinal section, HE stained. (f) Same as e, but with NrCAM$^{-/-}$. (g–h) 2-mo-old NrCAM$^{-/-}$ central longitudinal section, TB stained. (g) One-third of the way to the center side-front region. (h) Half-way to the center posterior region. (i–k) 8-mo-old NrCAM$^{-/-}$ lens in longitudinal noncentral section, HE stained. (i) Marginal region. (j) Anterior region. (k) Posterior region. *Cellular debris; arrowheads, intensely stained rounded cell; arrows, examples of secondary fiber cells in the process of rounding up due to contact loss of neighboring cells; open arrows, cells in the process of disintegration.

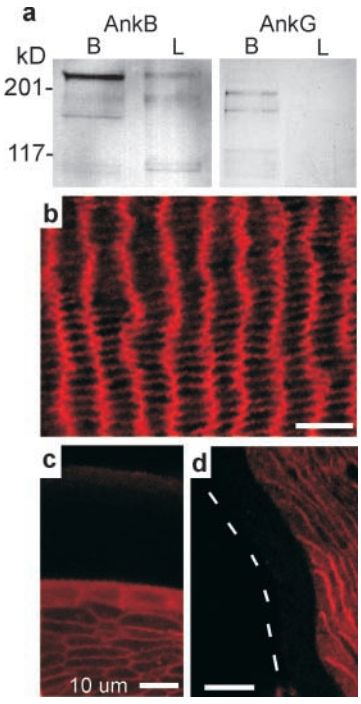

Figure 5. **Ankyrin-B but not -G is expressed in the lens.** (a) Immunoblot of brain and lens lysates using antibodies against ankyrin-B or -G. The molecular weight markers are indicated on the left. (b) Longitudinal noncentral section of 9-mo-old mouse lens stained with antibodies against ankyrin-B. (c) Same as b, but anterior region showing expression of ankyrin-B in the epithelium but not the capsule. (d) P12 longitudinal lens section showing that the lens fiber membranes neighboring the capsule do not express ankyrin-B. The capsule position is indicated.

To investigate the effect of the absence of ankyrin-B on the organization of F-actin, we performed phalloidin staining. Abnormal cellular arrangement at the anterior pole of 1-d-old ankyrin-B$^{-/-}$ mice was also detected using this staining method. In addition the stain was nonuniform and some F-actin aggregates were observed (Fig. 6 e, filled arrowheads). Consistently, similar cytoskeletal disturbances were observed in NrCAM$^{-/-}$ lenses at this stage (not shown). NrCAM was still targeted to the plasma membrane in ankyrin-B–deficient lenses, however, we observed a tendency to a more nonuniform membrane distribution in rounded lens cells (not shown).

Disorganization of F-actin and Connexin50 in NrCAM-deficient mice

At P12 abnormally shaped NrCAM$^{-/-}$ lens fibers also show irregularities in their F-actin, including some aggregates (Fig. 7 a, filled arrowheads). Other cells, mostly cells of the marginal zone that originated from dividing epithelial cells more recently, still show a normal uniform F-actin distribution below their membranes, resembling wild-type cells (Fig. 7 a, open arrowheads). By the age of 2.5 mo, the cataractous lens shows severe disorganization of the actin cytoskeleton, including F-actin aggregates below the entire membrane surface of rounded cells (Fig. 7 b, filled arrowheads). A normal F-actin arrangement only remains within cells very close to the marginal zone (Fig. 7 b, open arrowheads). The cellular debris as well as some lens fibers in the process of disintegration are devoid of F-actin (not shown). Ankyrin-B is capable of binding to spectrin, which in turn binds to actin. Consistently, the distribution of ankyrin-B in NrCAM-deficient

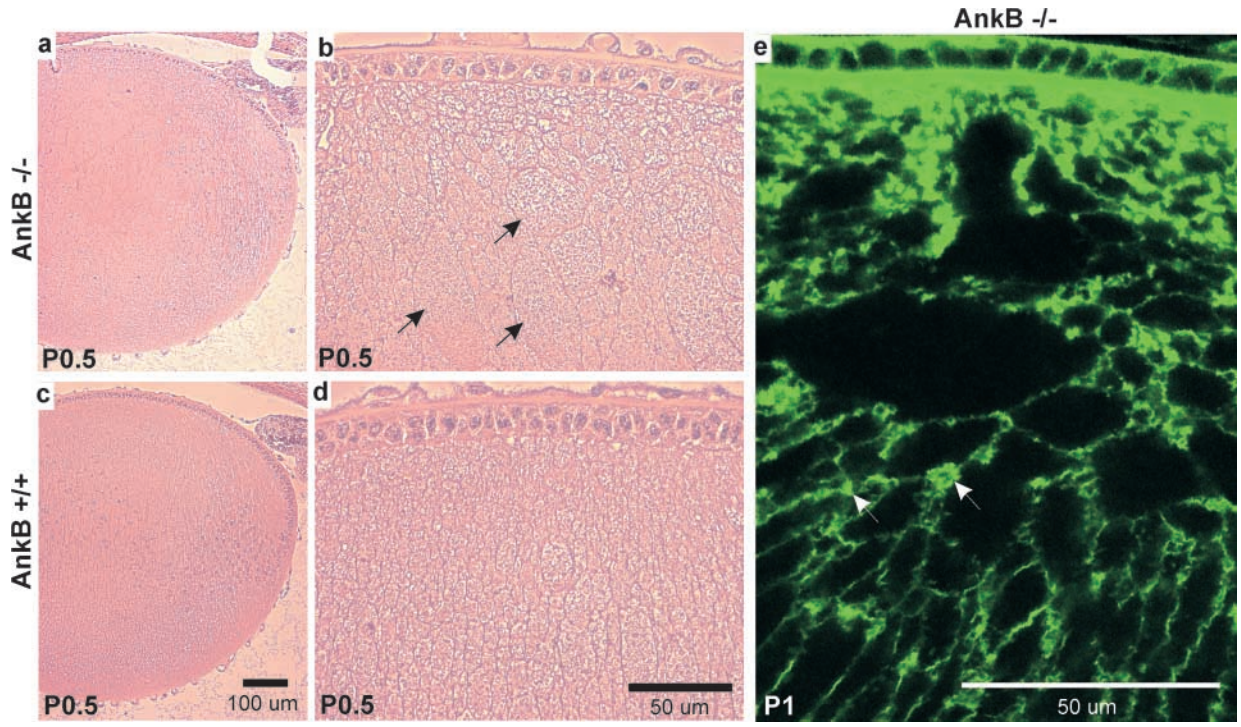

Figure 6. **The absence of ankyrin-B causes similar lens fiber disorganization as the absence of NrCAM.** (a and b) Longitudinal section through a P0.5 ankyrin-B$^{-/-}$ lens, HE stained. Arrows, rounded abnormal shaped cells. (c and d) Longitudinal section through a P0.5 ankyrin-B$^{+/+}$ sibling lens, HE stained. (e) Longitudinal section through a P1 ankyrin-B$^{-/-}$ lens, stained with the F-actin stain FITC-phalloidin. Arrows, aggregates of F-actin.

lenses resembled that of F-actin, including aggregate formation (not shown).

To examine the effect of the absence of NrCAM on gap junctions, we performed immunohistological stains using antibodies against connexin50. Although wild-type lenses have a regular arrangement of connexin50-containing gap junctions, 1-mo-old NrCAM-deficient lenses show a reduced number of these gap junctions especially towards inner layers of secondary lens fibers, and especially at the lens poles. In addition, we observe aggregates of connexin50, especially in the more interior layers of secondary lens fibers that have a higher occurrence of abnormally shaped cells. We conclude that NrCAM is not required for the localization of connexin50 to gap junctions when they are first created, but that it is required for gap junction maintenance, most likely indirectly by enabling cell–cell contact.

Axonal pathfinding in the spinal cord and neurite outgrowth of NrCAM$^{-/-}$ cells

Previous studies on NrCAM indicated a role for NrCAM in axonal pathfinding by in ovo antibody perturbation experiments (Stoeckli and Landmesser, 1995; Perrin et al., 2001). Therefore, we analyzed the growth of commissural axons and proprioceptive axons of the spinal cord by dye tracing and immunohistological studies. In DiI tracings of E11.5, E12.5, and E13.5, commissural axons, followed by open book preparations (Fig. 8, a and b), we found that commissural axons crossed the floor plate in NrCAM-deficient embryos as com-

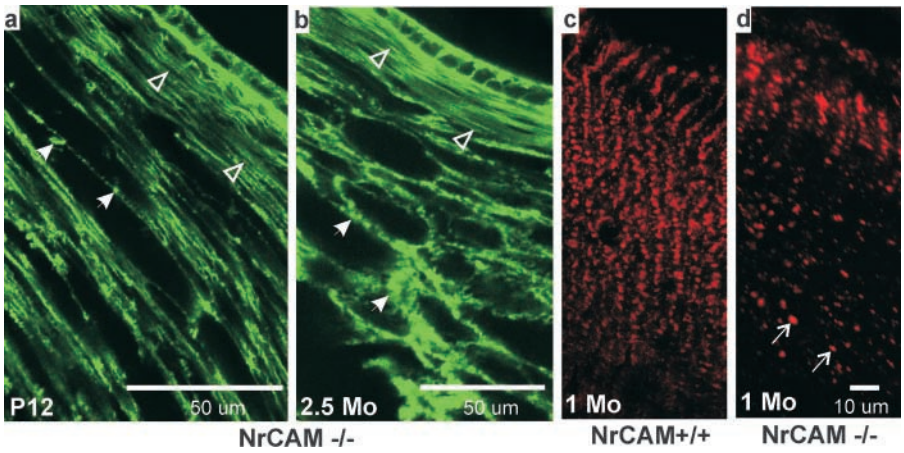

Figure 7. **Disorganization of F-actin and connexin50 in the absence of NrCAM.** (a and b) P12 and 2.5-mo-old, respectively, lateral-anterior longitudinal section through an NrCAM$^{-/-}$ lens, stained with FITC-phalloidin. Filled arrowheads, examples of F-actin aggregates; open arrowheads, examples of bordering cell membranes with a still normal ordered F-actin arrangement. (c and d) 1-mo-old lenses stained with monoclonal antibodies against the gap junctional protein connexin50. (c) wild type. (d) NrCAM$^{-/-}$. Arrows, connexin50 aggregates.

pletely, as in heterozygous or wild-type controls. In seven E11.5 NrCAM-deficient embryos, we counted 676 single fluorescent commissural axons, and only 10 of them showed an aberrant growth, in that they grew rostrally or caudally on the ipsilateral side of the floor plate for a short distance. However, 7 of these 10 axons still crossed the midline at a point more rostrally or caudally, and proceeded in the correct path after that. This amounts to a pathfinding error rate of 1.48%, a frequency comparable to that encountered in wild type (11 of 741 axons). Interestingly, significant pathfinding errors of commisural axons were also not observed in ankyrin-B–deficient mice (unpublished data).

One explanation of the slight motor defect observed for NrCAM$^{-/-}$ mice would be pathfinding errors of proprioceptive neurons in the spinal cord, since these neurons are responsible for sensing body positions. However, a selective stain of these axons in E15 embryos using antibodies against parvalbumin revealed no significant abnormalities (Fig. 8, c and d). Further histological studies within the developing nervous system including retina, cerebellum, and spinal cord using antibodies to various neural proteins do not reveal any gross anatomical defects within NrCAM mutant mice (not shown).

Previous cell culture analyzes using embryonal chicken tectal neurons show an inhibition of neurite growth on immobilized F11 or neurofascin (Morales et al., 1993; Volkmer et al., 1996) by NrCAM antibodies, indicating that NrCAM acts as neuronal receptor protein for these substrates. Furthermore, if TN-R is complexed with F11 or neurofascin, β_1 integrins and at least one additional protein are used as receptors (Volkmer et al., 1998; Zacharias et al., 1999). To analyze these observations further, embryonic brains of control or NrCAM$^{-/-}$ mice were dissociated, and single cells were seeded on a surface coated with substrate proteins. After 24-h incubation, NrCAM$^{-/-}$ neurite formation was absent or almost absent on F11 or neurofascin (Fig. 8, i and l), resembling the situation on uncoated culture dishes (Fig. 8, e and f), whereas wild-type neurons extended long neurites on F11 or neurofascin (Fig. 8, h and k). As expected, growth on poly-L-lysine or laminin-1 (not shown) was unaffected by the mutation. When F11 or neurofascin-coated surfaces were complexed with tenascin-R NrCAM-deficient neurons were able to extend neurites similar to wild-type neurons (Fig. 8, j and m; not shown). No neurite growth of NrCAM$^{-/-}$ neurons was detected on surfaces blocked with BSA and subsequently incubated with TN-R (Fig. 8 g), or on surfaces coated with F11 or neurofascin and blocked with BSA (not shown). These results confirm our previous cell culture observations with chicken neurons in antibody perturbation experiments.

Discussion

NrCAM, previously not known to be expressed in the lens, is essential for maintenance of lens transparency and an ordered arrangement of lens fiber cells. Interestingly, the absence of ankyrin-B causes similar lens fiber disorganization as the absence of NrCAM, and both mutations cause cytoskeletal disarrangement, providing a genetic link between the interaction of NrCAM and ankyrin-B. Unexpectedly, significant pathfinding errors of commissural axons at the midline and of proprioceptive collaterals of the spinal cord are not detectable in the absence of NrCAM. NrCAM and other L1 subfamily members and their ligands are expressed in the developing nervous system in a dynamic and partially overlapping pattern (Brümmendorf and Rathjen, 1995; Brümmendorf et al., 1998). In contrast, only NrCAM, but none of its

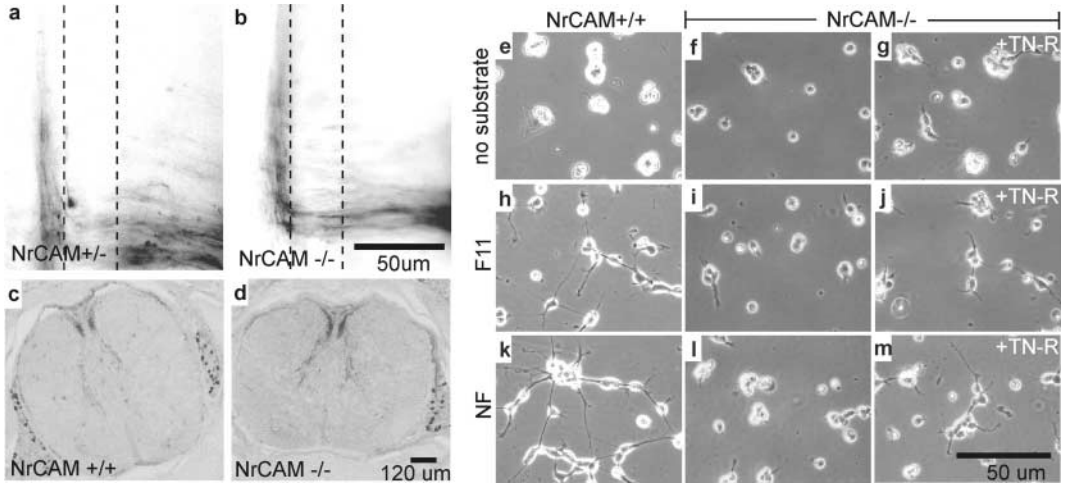

Figure 8. **Analysis of axonal pathfinding and neurite extension.** In NrCAM-deficient mice, commissural axons cross the spinal cord midline (floor plate) as efficiently as in wild type. Rostral is up. (a and b) Open book preparations of DiI tracing of E12.5 commissural axons. (a) Heterozygote. (b) NrCAM$^{-/-}$. The broken lines indicate the location of the floor plates. (c and d) Immunostains of E15 proprioceptive neurons in forelimb region of the spinal cord using antibodies against parvalbumin reveal no differences in the pathfinding of proprioceptive collaterals. (c) Wild-type. (d) NrCAM$^{-/-}$. (e–m) 24-h neurite outgrowth of whole brain embryonal neurons. Unlike wild type, NrCAM-deficient neurons are unable to grow on the subtrates F11 or neurofascin (NF). However, they can grow on the complexes F11–tenascin-R or NF–tenascin-R (TN-R), since instead of NrCAM β_1 integrins and at least one additional protein are used as receptors. (e, h, and k) E12 wild-type neurons. (f, g, i, j, l, and m) NrCAM$^{-/-}$ neurons. (e and f) No substrate. (g) Surface blocked with BSA, followed by incubation with TN-R before neuron seeding. (h and i) F11 as substrate. (j) F11 as substrate, then BSA blockage and TN-R treatment. (k and l) Neurofascin-Fc as substrate. (m) Neurofascin-Fc as substrate, then BSA blockage and TN-R treatment.

family members nor its ligands, are expressed in the lens. Thus, no other family member can compensate a loss of NrCAM in these cells. This might be the reason for this deleterious effect on the structure of lens fibers caused by the absence of NrCAM in contrast to the situation within the developing nervous system.

It is likely that the lens phenotype results from a perturbation of the maintenance of contacts between lens fiber cells. The absence of the currently known ligands of NrCAM suggests that this contact is mediated by homophilic binding of NrCAM on lens fibers. The consequences of the lack to establish appropriate contacts between cell membranes may result in the failure to form water channels by aquaporins or gap junctions, as indicated here by the irregular distribution and decrease of connexin50-containing gap junctions. Water channels and gap junctions are important for the transport of water or ions, metabolites, and second messengers and allow communication between metabolically inert lens fibers deep within the lens. Gap junctional channels that bridge the extracellular space are formed by members of the connexin gene family, in particular in lenses, by connexin50, -46, and -43, that allow transport of small molecules and facilitate the continuous flow (<1 kD) of ions, metabolites, and second messengers. This flow appears to be important for lens clarity, as demonstrated by analysis of connexin50 and -46 mutant mice (Gong et al., 1997; White et al., 1998) and mutations in humans (Shiels et al., 1998; Mackay et al., 1999). The absence of connexin50 in mice results in reduced growth of the lens and the eye and the appearance of zonular pulverulent nuclear cataracts, however intercellular communication is not completely lost in these mice. In the absence of connexin50, lenses develop a nuclear cataract that is associated with the proteolysis of crystallins. Mutations within the major intrinsic protein, which also is important for intercellular communication of the lens fibers, causes lamellar cataracts in humans and mice (Shiels and Bassnett, 1996; Berry et al., 2000). The major intrinsic protein that forms tetramers within the plasma membrane regulates the transport of water in an energy- and direction-independent manner (Heymann et al., 1998). Other mutations in humans or mice known to cause cataracts include genes encoding crystallins, which constitute the main cytoplasmic proteins in lens and the transcription factor PITX3 (Semina et al., 1998; Francis et al., 1999; Graw, 1999).

As shown by lens fiber disorganization in the ankyrin-B$^{-/-}$ lens, NrCAM function requires a link to the cytoskeleton via ankyrin. In addition, the transmembrane protein NrCAM, as well as the cytoskeletal linker protein ankyrin-B may function directly in maintaining an ordered cytoskeleton in the lens, for example, by anchoring the cytoskeleton to the lens membrane. Alternatively or in addition, the observed disarrangement of F-actin may be caused indirectly due to the perturbed lens metabolism. Both NrCAM and ankyrin-B, but most likely the cytoskeleton as a whole, may also be important for the suprastructural organization of cytoplasmic proteins such as the crystallins. Thus, crystallins might not be able to maintain their normal organization in NrCAM-deficient lenses, thus creating opacification.

Although the *NrCAM* (human chromosome 7q22-31) (Burmeister et al., 1996; Lane et al., 1996) and *ankyrin-B* (human chromosome 4q25-q27) (Tse et al., 1991) loci have not been mapped so far to cataract formation in humans, our studies in mice might contribute to the understanding of cataract formation in humans. NrCAM is very similar to L1, the founder of this subfamily of adhesion proteins within the Ig superfamily. Missense mutations within the L1 gene have been shown to result in a broad spectrum of neurological disorders with different degrees of severity (Wong et al., 1995; Brümmendorf et al., 1998). It is conceivable that point mutations within the NrCAM gene affecting its homophilic binding activity might also cause cataract formation to different degrees. It is therefore not unlikely to implicate the NrCAM gene in recessive forms of inherited human cataracts. In addition, the inherited deletion or mutation of one *NrCAM* or *ANK2* allele could increase the susceptibility to age-related cataract formation. An inherited complete absence of ankyrin-B, however, might be lethal at early stages, as observed for mice (Scotland et al., 1998).

Materials and methods

Mapping the *NrCAM* locus and derivation of mutant mice

To obtain information about the mouse *NrCAM* locus, a PCR screen in a mouse ES BAC library was done using primers derived from rat cDNA sequence of NrCAM. Probes for mapping were created by PCR, using the rat cDNA sequence information for the primer design, and mouse genomic DNA for template. The BAC clone was mapped using 15 common restriction enzymes, and a long and short arm was subcloned from it. The short arm (EMBL/GenBank/DDBJ accession no. AF346472) consists of the 600-bp (PvuII-PvuII) fragment just upstream of the NrCAM exon containing the ATG (exon 4). The long arm consists of the NheI-SpeI 6-kb fragment, containing DNA from 1 kb downstream of exon 4 (NheI) to 0.5 kb downstream of exon 7 (SpeI). Short and long arms were inserted into the bluescript-derived vector pTG1 (Atugen) containing a neo cassette and TK. The targeting vector was electroporated into E14.1 ES cells (129/ola) and screened by PCR screen (using neoL1 5′-CCTGCGTGCAATCCATCTTGTTCAATG-3′ and Moré1 5′-GAATAGATCAGTCGGGTCACTGAGG-3′). Blastocyst injection and transfer into pseudopregnant foster mice were done by Atugen. 14 chimeric mice derived from one ES cell clone were obtained, of which 5 were germline chimeras. The chimeras were crossed with C57/BL6 mice, and the resulting heterozygous animals were crossed with each other to obtain homozygous mice. Genotyping of the mice was done by PCR using Taq polymerase (GIBCO BRL) and the above primers for detection of the disrupted allele as well as Moré1 combined with Mimo71 (5′-CAGGAAGAGAATCAGGGGCACTC-3′) for detection of the wild-type allele. Alternatively, genomic Southern blotting was performed using a digoxygenin-labeled SacI-NheI fragment as external probe. The correct integration of the targeting vector was confirmed using a Dig-labeled PauI-NheI fragment (region deleted in the mutant) as probe (not shown).

Generation of polyclonal antibodies against NrCAM and immunoblot analysis

The rat cDNA clone number 22 of NrCAM (obtained from V. Bennett, Duke University, Durham, NC) was used to create a DNA fragment coding for NrCAM FNIII domains 1–4 via PCR, using Pfu polymerase, MIMO62 5′-CGGGATCCGCAGCCAACACAACGCTGGACAGT-3′, and MIMO50 5′-CGGAATTCGCCTGCACCTACATCAGGTGGAAGA-3′. The fragment was digested with EcoRI and BamHI and cloned into pGEX-6P-1 (Amersham Pharmacia Biotech), and then cloned into pQE30 (QIAGEN) using BamHI and SalI to create pMIM463. His-tagged NrCAM was expressed and purified under denaturing conditions according to the manufacturers' instructions (QIAGEN and CLONETECH Laboratories, Inc. [TALON metal affinity resin]). One rabbit was immunized with doses of 100 μg of renatured purified protein, first in complete Freund's adjuvants, followed every second week by a dose in incomplete Freund's adjuvants. Serum of the immunized rabbit was applied to protein A–Sepharose (Amersham Pharmacia Biotech) to purify the IgG fraction, followed by affinity purification on nitrocellulose-immobilized NrCAM.

For the immunoblots, tissue was homogenized in RIPA buffer (1 M NaCl, 0.02 M EDTA, 0.1% SDS, 1% Triton X-100, 1 M Tris, pH 7.4) con-

taining protease inhibitors. Laemmli SDS-PAGE buffer was added, and samples were boiled for 5 min and centrifuged. The supernatant was used for SDS-PAGE (one lane containing the soluble fraction from 4 mg of tissue). After electrophoresis, the proteins were blotted onto nitrocellulose. In the first antibody reaction, 10 μg/ml 463 antibody were used. The secondary antibody was 0.25 μg/ml goat anti–rabbit alkaline phosphatase antibody (Dianova). For antiankyrin immunoblots, cytoskeletal proteins were extracted by high salt before SDS-PAGE.

Animal handling, documentation of mouse growth, and motor ability

For the growth curves, a male NrCAM$^{-/-}$ mouse was mated with a female NrCAM$^{+/-}$ mouse, resulting a large litter of 12 pups. The pups were marked and weighed at various time points.

For the rotarod test, a plastic rotarod inside a large box was used, driven by a small electric engine. Female mice weighing 13.8–14.3 g on average for NrCAM$^{-/-}$ and slightly younger control mice, respectively, were confronted without prior rod experience first with the nonmoving rod; and after a recovery time with the rod, rotating at 6.5 rpm. The number of times the animals fell from the rod in 3 min was counted, and animals were put back onto the rod immediately after each fall. Mice were genotyped after the experiment.

DiI tracing of commissural axons in the spinal cord

E11.5, E12.5, and E13.5 embryos of NrCAM$^{+/-}$ and NrCAM$^{-/-}$ mixed litters were fixed in 4% paraformaldehyde (PFA)/PBS overnight. The spinal cord was exposed by removing overlying tissue. A saturated solution of DiI in ethanol was injected through a filament-containing pulled-out glass injection needle into the lateral spinal cord. Generally, 3–4 injections were done per spinal cord, spaced out over it's entire length. Tracing was done for 2.5 d at 37°C in 4% PFA/PBS, followed by an open book preparation of the spinal cord (Stoeckli and Landmesser, 1995). Tracings were viewed under a fluorescence microscope and documented using an Axiocam digital camera (ZEISS). Images were converted to black and white and inverted using Adobe® Photoshop™.

Histological examinations

10–14 μm cryostat sections (using a Leica cryostat) were done on tissues previously fixed in 4% PFA/PBS and equilibrated in 30% sucrose/PBS. For immunohistology, the sections were blocked with 10% normal goat serum, 0.1% BSA/PBS, and incubated with the primary antibody (5–10 μg/ml in blocking solution, for 2 h at room temperature (RT) or overnight at 4°C). After several PBS washing steps, secondary antibody (3 μg/ml goat anti–rabbit Cy3 or rabbit anti–mouse Cy3; Dianova) was applied for 2 h at RT, followed by several PBS washes. Fluorescence images were documented using a fluorescence microscope and a confocal scanning microscope (Bio-Rad Laboratories). Monoclonal antibody against connexin50 was obtained from Zytomed.

For phalloidin stains, sections were blocked with 0.2% BSA/PBS and incubated with the (1 μg/ml) FITC–phalloidin for 30 min. After several TBS/0.1% Triton X-100 washing steps, fluorescence images were documented using a fluorescence microscope and the confocal scanning microscope.

For JB4 sections (Polysciences, Inc.), whole eyes were fixed in 75% ethanol/25% acetic acid, dehydrated in 100% ethanol, and embedded using the manufacturer's instructions. 1-μm sections were done using a semithin microtome (model HM360; Microm). The sections were stained using toluidine blue (TB) or hematoxylin/eosin (HE) stain and documented using a microscope with phase–contrast setting and an Axiocam digital camera (ZEISS).

Neurite outgrowth assays

Under sterile conditions, eight-well chamber slide gaskets (Lab-Tek) were attached to hydrophobic petriPERM dishes (Heraeus). The proteins F11, neurofascin-Fc (isoform 15), and TN-R were purified as described elsewhere (Volkmer et al., 1996; Zacharias et al., 1999). Wells were coated with 100 μl of PBS containing 10 μg of substrate and incubated overnight at 4°C in a moist atmosphere. To obtain substrate–TN-R complexes, the primary substrate was first blocked with 100 μg/ml BSA in PBS for 1 h at RT. This was followed by a PBS wash and an incubation with 5 μg/ml TN-R in PBS for 4 h at RT.

Mouse neurons were prepared from E12 total brains using a published protocol and were seeded onto the prepared substrate-binding petriperm surfaces in neurobasal medium (GIBCO BRL) (containing the additives B27, glutamine, and penicillin/streptomycin) at a concentration of 20,000 cells/well. Neurite outgrowth was documented using phase–contrast microscopy and an Axiocam digital camera after 24 h of incubation at 37°C under cell culture conditions.

The authors are grateful to V. Bennett for providing us with rat NrCAM cDNA clones, as well as with antibodies against ankyrin-B and -G, and most of all, ankyrin-B$^{+/-}$ mice. We thank M. Richter and M. Schachner for antibodies against CHL1, M. Grumet for antibodies against NrCAM, R.U. Margolis and A. Faissner for antibodies against RPTPβ/ζ. We are grateful for the expert technical help of Y. Klosowski and advice of L. Li, A. Garratt, and C. Birchmeier concerning the analysis of mutant mice. Thanks to G. Lewin for the introduction into DiI tracing and to F. Pfrieger and I. Haupt for the introduction into the mouse neuron cell culture technique. We thank J. Graw and D.C. Beebe for their helpful discussions and advice concerning cataracts and acknowledge the critical reading of the manuscript by J. Graw, M. Koroll, K. Sharma, A. Garratt, and U. Zacharias. We thank S. Kenwrick for information on the human NrCAM location prior publication.

This work was supported by DFG grant SFB515 to F.G. Rathjen, and a Liebig habilitation stipend of the Verband der Chemischen Industrie to M.I. Moré.

Submitted: 10 April 2001
Revised: 23 May 2001
Accepted: 4 June 2001

References

Bassnett, S., H. Missey, and I. Vucemilo. 1999. Molecular architecture of the lens fiber cell basal membrane complex. *J. Cell Sci.* 112:2155–2165.

Berry, V., P. Francis, S. Kaushal, A. Moore, and S. Bhattacharya. 2000. Missense mutations in MIP underlie autosomal dominant 'polymorphic' and lamellar cataracts linked to 12q. *Nat. Genet.* 25:15–17.

Brümmendorf, T., and F.G. Rathjen. 1995. Cell adhesion molecules 1: immunoglobulin superfamily. *Prot. Profile.* 2:963–1108.

Brümmendorf, T., S. Kenwrick, and F.G. Rathjen. 1998. Neural cell recognition molecule L1: from cell biology to human hereditary brain malformations. *Curr. Opin. Neurobiol.* 8:87–97.

Burmeister, M., Q. Ren, G.J. Makris, D. Samson, and V. Bennett. 1996. Genes for the neuronal immunoglobulin domain cell adhesion molecules neurofascin and Nr-CAM map to mouse chromosomes 1 and 12 and homologous human chromosomes. *Mamm. Genome.* 7:558–559.

Cohen, N.R., J.S. Taylor, L.B. Scott, R.W. Guillery, P. Soriano, and A.J. Furley. 1998. Errors in corticospinal axon guidance in mice lacking the neural cell adhesion molecule L1. *Curr. Biol.* 8:26–33.

Dahme, M., U. Bartsch, R. Martini, B. Anliker, M. Schachner, and N. Mantei. 1997. Disruption of the mouse L1 gene leads to malformations of the nervous system. *Nat. Genet.* 17:346–349.

Davis, J.Q., and V. Bennett. 1994. Ankyrin binding activity shared by the neurofascin/L1/NrCAM family of nervous system cell adhesion molecules. *J. Biol. Chem.* 269:27163–27166.

De Angelis, E., J. MacFarlane, J.S. Du, G. Yeo, R. Hicks, F.G. Rathjen, S. Kenwrick, and T. Brümmendorf. 1999. Pathological missense mutations of neural cell adhesion molecule L1 affect hemophilic and heterophilic binding activities. *EMBO J.* 18:4744–4753.

Demyanenko, G.P., A.Y. Tsai, and P.F. Maness. 1999. Abnormalities in neuronal process extension, hippocampal development, and the ventricular system of L1 knockout mice. *J. Neurosci.* 19:4907–4920.

Dola, A., M. Katar, P. Hussain, and H. Maisel. 1990. Ankyrin of the ocular lens. *Ophthalmic Res.* 22:295–301.

Dry, K., S. Kenwrick, A. Rosenthal, and M. Platzer. 2001. The complete sequence of the human locus for NrCAM (NgCAM-related cell adhesion molecule) reveals a novel alternative exon in chick and man and conserved genomic organisation for the L1 subfamily. *Gene.* In press.

Fitzli, D., E.T. Stoeckli, S. Kunz, K. Siribour, C. Rader, B. Kunz, S.V. Kozlov, A. Buchstaller, R.P. Lane, D.M. Suter, W.J. Dreyer, and P. Sonderegger. 2000. A direct interaction of axonin-1 with NgCAM–related cell adhesion molecule (NrCAM) results in guidance, but not growth of commissural axone. *J. Cell Biol.* 149:951–968.

Francis, P.J., V. Berry, A.T. Moore, and S. Bhattacharya. 1999. Lens biology: development and human cataractogenesis. *Trends Genet.* 15:191–196.

Francis, P.J., V. Berry, S.S. Bhattacharya, and A.T. Moore. 2000. The genetics of childhood cataract. *J. Med. Genet.* 37:481–488.

Gong, X., E. Li, G. Klier, Q. Huang, Y. Wu, H. Lei, N.M. Kumar, J. Horwitz, and

N.B. Gilula. 1997. Disruption of alpha3 connexin gene leads to proteolysis and cataractogenesis in mice. *Cell*. 91:833–843.

Graw, J. 1999. Cataract mutations and lens development. *Prog. Retin. Eye Res*. 18: 235–267.

Grumet, M., V. Mauro, M.P. Burgoon, G.M. Edelman, and B.A. Cunningham. 1991. Structure of a new nervous system glycoprotein, Nr-CAM, and its relationship to subgroups of neural cell adhesion molecules. *J. Cell Biol.* 113: 1399–1412.

Heymann, J.B., P. Agre, and A. Engel. 1998. Progress on the structure and function of aquaporin 1. *J. Struct. Biol.* 121:191–206.

Hortsch, M. 2000. Structural and functional evolution of the L1 family: are four adhesion molecules better than one? *Mol. Cell Neurosci.* 15:1–10.

Jefford, G., and R.R. Dubreuil. 2000. Receptor clustering drives polarized assembly of ankyrin. *J. Biol. Chem.* 275:27726–27732.

Kayyem, J.F., J.M. Roman, E.J. de la Rosa, U. Schwarz, and W.J. Dreyer. 1992. Bravo/Nr-CAM is closely related to the cell adhesion molecules L1 and Ng-CAM and has a similar heterodimer structure. *J. Cell Biol.* 118:1259–1270.

Lambert, S., J.Q. Davis, and V. Bennett. 1997. Morphogenesis of the node of Ranvier: co-clusters of ankyrin and ankyrin-binding integral proteins define early developmental intermediates. *J. Neurosci*. 17:7025–7036.

Lane, R.P., X.N. Chen, K. Yamakawa, J. Vielmetter, J.R. Korenberg, and W.J. Dreyer. 1996. Characterization of a highly conserved human homolog to the chicken neural cell surface protein Bravo/Nr-CAM that maps to chromosome band 7q31. *Genomics*. 35:456–465.

Mackay, D., A. Ionides, Z. Kibar, G. Rouleau, V. Berry, A. Moore, A. Shiels, and S. Bhattacharya. 1999. Connexin46 mutations in autosomal dominant congenital cataract. *Am. J. Hum. Genet.* 64:1357–1364.

Mauro, V.P., L.A. Krushel, B.A. Cunningham, and G.M. Edelman. 1992. Homophilic and heterophilic binding activities of Nr-CAM, a nervous system cell adhesion molecule. *J. Cell Biol.* 119:191–202.

Morales, G., M. Hubert, T. Brümmendorf, U. Treubert, A. Tarnok, U. Schwarz, and F.G. Rathjen. 1993. Induction of axonal growth by heterophilic interactions between the cell surface recognition proteins F11 and NrCAM/Bravo. *Neuron*. 11:1113–1122.

Moulding, H.D., R.L. Martuza, and S.D. Rabkin. 2000. Clinical mutations in the L1 neural cell adhesion molecule affect cell-surface expression. *J. Neurosci.* 20:5696–5702.

Perrin, F.E., F.G. Rathjen, and E. Stoeckli. 2001. Distinct subpopulations of sensory afferents require F11 or axonin-1 for growth to their target layers within the spinal cord of the chick. *Neuron*. In press.

Sakurai, T., M. Lustig, M. Nativ, J.J. Hemperly, J. Schlessinger, E. Peles, and M. Grumet. 1997. Induction of neurite outgrowth through contactin and Nr-CAM by extracellular regions of glial receptor tyrosine phosphatase β. *J. Cell Biol.* 136:907–918.

Scotland, P., D. Zhou, H. Benveniste, and V. Bennett. 1998. Nervous system defects of $Ankyrin_B$ (-/-) mice suggest functional overlap between the cell adhesion molecule L1 and 440-kD $Ankyrin_B$ in premyelinated axons. *J. Cell Biol*. 143:1305–1315.

Semina, E.V., R.E. Ferrell, H.A. Mintz-Hittner, P. Bitoun, W.L. Alward, R.S. Reiter, C. Funkhauser, H.S. Daack, and J.C. Murray. 1998. A novel homeobox gene PITX3 is mutated in families with autosomal-dominant cataracts and ASMD. *Nat. Genet*. 19:167–170.

Shiels, A., and S. Bassnett. 1996. Mutations in the founder of the MIP gene family underlie cataract development in the mouse. *Nat. Genet*. 12:212–215.

Shiels, A., D. Mackay, A. Ionides, V. Berry, A. Moore, and S. Bhattacharya. 1998. A missense mutation in the human connexin50 gene (GJA8) underlies autosomal dominant "zonular pulverulent" cataract, on chromosome 1q. *Am. J. Hum. Genet.* 62:526–532.

Stoeckli, E.T., and L. Landmesser. 1995. Axonin-1, Nr-CAM, and Ng-CAM play different roles in the in vivo guidance of chick commissural neurons. *Neuron*. 14:1165–1179.

Suter, D.M., G.E. Pollerberg, A. Buchstaller, R.J. Giger, W.J. Dreyer, and P. Sonderegger. 1995. Binding between the neural cell adhesion molecules axonin-1 and nr-cam/bravo is involved in neuron-glia interaction. *J. Cell Biol.* 131:1067–1081.

Tse, W.T., J.C. Menninger, T.L. Yang-Feng, U. Francke, K.E. Sahr, S.E. Lux, D.C. Ward, and B.G. Forget. 1991. Isolation and chromosomal localization of a novel nonerythroid ankyrin gene. *Genomics*. 10:858–866.

Tuvia, S., T.D. Garver, and V. Bennett. 1997. The phosphorylation state of the FIGQY tyrosine of neurofascin determines ankyrin-binding activity and patterns of cell segregation. *Proc. Natl. Acad. Sci. USA*. 94:12957–12962.

Volkmer, H., R. Leuschner, U. Zacharias, and F.G. Rathjen. 1996. Neurofascin induces neurites by heterophilic interactions with axonal NrCAM while Nr-CAM requires F11 on the axonal surface to extend neurites. *J. Cell Biol*. 135: 1059–1069.

Volkmer, H., U. Zacharias, U. Nörenberg, and F.G. Rathjen. 1998. Dissection of complex molecular interactions of neurofascin with Axonin-1, F11, and Tenascin-R, which promote attachment and neurite formation of tectal cells. *J. Cell Biol*. 142:1083–1093.

White, T.W., D.A. Goodenough, and D.L. Paul. 1998. Targeted ablation of connexin50 in mice results in microphthalmia and zonular pulverulent cataracts. *J. Cell Biol*. 143:815–825.

Wong, E.V., S. Kenwrick, P.J. Willems, and V. Lemmon. 1995. Mutations in the cell adhesion molecule L1 cause mental retardation. *Trends Neurosci.* 18: 168–172.

Zacharias, U., U. Nörenberg, and F.G. Rathjen. 1999. Functional interactions of the immunoglobulin superfamily member F11 are differentially regulated by the extracellular matrix proteins Tenascin-R and Tenascin-C. *J. Biol. Chem*. 274:24357–24365.